



WEDNESDAY SLIDE CONFERENCE 2008-2009

Conference 25

13 May 2009

Conference Moderator:

Jo Lynne Raymond, DVM, Diplomate ACVP

CASE I – 07-59363 (AFIP 3121220)

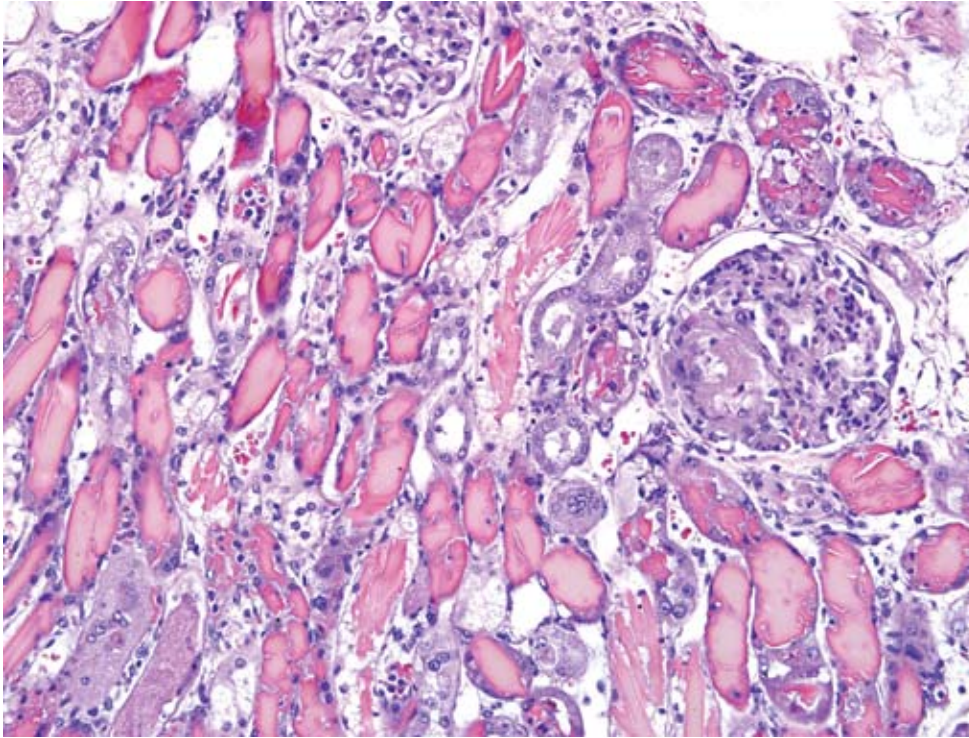
Signalment: 4-year-old, male castrated, Italian greyhound breed canine (*Canis familiaris*)

History: This dog presented to the critical care service with a primary complaint from the referring veterinarian of possible toxicity and/or multi-organ failure. The owner reported that the night before presentation, the dog had vomited 18 times, and that since then the dog was listless and weak, and had not urinated since the onset of clinical signs. The dog was housed with three other dogs, including one who exhibited vomiting and diarrhea three days prior to this dog's illness but had recovered uneventfully.

Gross Pathology: Autolysis was moderate. The right and left kidneys were diffusely purple-black, and the urinary bladder contained approximately 1 ml of dark red urine. Petechial hemorrhages were present on visceral pleural surfaces of all lung lobes, and there was mild pulmonary edema. The peritoneal cavity contained approximately 150 ml of serosanguineous fluid. The entire gastrointestinal tract from stomach to rectum contained scant, tenacious, brown-black material resembling digested blood. The spleen was contracted, with an absence of blood in the red pulp.

Laboratory Results: At presentation to the teaching hospital the dog's hematocrit was 5% (37-55), white blood cell count was $51.7 \times 10^3/\text{ul}$ (6-17) (95% neutrophils, no bands), hemolysis index 2567 (3-56), creatinine was 6.9 mg/dl (0.6-1.4), and blood urea nitrogen was 185 mg/dl (12-26). The dog was anuric, and no urine was available for diagnostic testing. A Coomb's test was not performed on this patient.

Histopathologic Description: Diffusely, most cortical distal tubules, collecting ducts, and medullary tubules contain extensive intraluminal casts (**Fig. 1-1**). Fewer casts are present in cortical proximal tubules. The majority of casts consist of amorphous to elongate crystalline, brightly eosinophilic material (hemoglobin casts) with fewer casts composed of eosinophilic, amorphous, globular or granular material variably admixed with sloughed epithelial cells (hyaline, cellular or granular casts). Less severely affected tubules within the cortex contain globular proteinaceous debris. When viewed with polarized light, casts contain small numbers of refractile, white, acicular, $5\mu\text{m} \times 20\text{-}30\mu\text{m}$ crystals. The epithelium lining these tubules is in various stages of degeneration, necrosis, and early regeneration, characterized by cells that are markedly attenuated, hyper eosinophilic with pyknotic or karyorrhectic nuclei,



1-1. Kidney, dog. Multifocally occluding tubules are numerous red-orange hyaline casts and fewer eosinophilic granular casts. Tubular epithelium is multifocally degenerative, necrotic, or regenerative. Capillary loops within glomeruli are occasionally occluded by fibrin thrombi and there is mild membranoproliferative glomerulonephritis. The cortical interstitium is multifocally expanded by edema. (HE 200X)

or sloughed into the tubular lumen (degeneration and necrosis). Some cells display anisocytosis, anisokaryosis, aggregation, hyperchromatic nuclei and occasional mitoses (regeneration). Scattered tubular epithelial cells contain brown granular cytoplasmic pigment. The tubular basement membrane is multifocally disrupted, and the adjacent interstitium is mildly edematous and has a mild interstitial infiltrate of neutrophils. Glomeruli diffusely have moderate amounts of proteinaceous material within Bowman's space. Within the vasa recta, there is variable congestion and neutrophilic leukostasis.

Contributor's Morphologic Diagnosis: Tubular epithelial degeneration and necrosis, acute, diffuse, severe, with regeneration, and marked intratubular hemoglobin, hyaline, and granular cast formation, consistent with hemoglobinuric nephrosis, kidney, Italian greyhound breed canine

Contributor's Comment: Clinical pathology data for this patient suggests an acute intravascular hemolysis, likely secondary to autoimmune mechanisms. The proximal tubular necrosis, in conjunction with the dramatic, widespread accumulation of obstructive hemoglobin casts, is consistent with peracute primary hemoglobin toxicity. Primary hemoglobin nephrotoxicity has a controversial role in veterinary medicine, although it is widely recognized in human medicine as a common and serious postoperative complication following

cardiopulmonary bypass¹ and, less commonly, in certain envenomations. Two diverging theories hold that hemoglobin is 1) not a direct nephrotoxin, but rather induces renal damage by a combination of hemoglobin-induced hypotension, increased vascular resistance, and disseminated intravascular coagulation resulting in renal ischemia; or 2) that hemoglobin is not directly toxic, but is converted to toxic byproducts within the urinary space, thereby inducing tubular necrosis.³ In experimental studies utilizing intravenously administered purified hemoglobin in rats, Zager et. al.³ concluded that hemoglobin can act as a primary nephrotoxin only in the presence of aciduria, and that the likely mechanism for this is aciduria-dependent conversion of hemoglobin to methemoglobin, the latter of which precipitates within distal tubule segments and forms casts. Unlike hemoglobin, once methemoglobin forms its precipitation can occur under either aciduric or alkaline conditions, and is more toxic than hemoglobin under either condition. Furthermore, distal tubular obstruction can lead to enhanced "upstream" uptake of hemoglobin and its metabolites by proximal tubules.³ Tubular damage in this case likely resulted from both local and systemic contributing factors, including massive, widespread tubular obstruction and attendant tubular epithelial necrosis, hypoxia secondary to the markedly decreased hematocrit, and hemoglobin-induced vasoconstriction via activation of the renin-angiotensin and sympathetic nervous system.²

The patient had mildly to moderately elevated D-dimers and partial thromboplastin time, but normal prothrombin time and no clinical evidence of bleeding. Calculation of the lipemia, free hemoglobin, and bilirubin is performed on a clinical chemistry analyzer by passing light of different wavelengths through the serum or plasma and calculating the amount of each interfering substance based on the light absorption of the sample. The amount of free hemoglobin is reported as the hemolysis index in units of mg/dL. Elevations as high as those present in this case can falsely decrease bicarbonate, GGT, amylase, and alkaline phosphatase, and can falsely increase AST, CK, iron, phosphate, triglycerides, magnesium, and total protein.

AFIP Diagnosis: Kidney: Tubular degeneration, necrosis, and regeneration, diffuse, marked with hemoglobin and granular casts and rare glomerular fibrin thrombi

Conference Comment: Acute renal failure is often caused by acute tubular necrosis. Acute tubular necrosis is usually caused by either nephrotoxic agents from the bloodstream, ischemia, or complete urinary outflow obstruction. The anatomic locations most susceptible to acute tubular necrosis are the proximal convoluted tubule and the thick ascending limb of the loop of Henle. This is in direct correlation to their high metabolic activity thus making them more susceptible to damage and necrosis.²

Ischemic tubular necrosis usually follows profound shock, and the extreme decrease in blood flow to the kidney results in renal cortical necrosis. The histologic hallmark of ischemic acute tubular necrosis is necrosis of the proximal, and to a lesser extent, distal tubules with disruption of tubular basement membranes and plugging of tubular lumina by casts. If the basement membrane is extensively damaged, then regeneration is impossible and the prognosis becomes grave.²

Nephrotoxic acute tubular necrosis causes necrosis of the proximal convoluted tubule because of the PCT's exposure to more toxin than the rest of the nephron as well as its high metabolic activity. The basement membrane is normally preserved in cases of nephrotoxic acute tubular necrosis providing scaffolding for cells to regenerate thus making the prognosis much more favorable than ischemic acute tubular necrosis.²

During the conference, several causes of tubular necrosis were discussed. Aminoglycosides, tetracyclines, sulfonamides, and the antifungal agent amphotericin B can cause tubular necrosis in domestic animals.² Ethylene glycol is also a common cause of tubular necrosis in dogs and cats. Oxalate containing plants including *Halgeton*

glomeratus (halogeton), *Sarcobatus vermiculatus* (greasewood), *Rheum rhaponticum* (rhubarb) are a few of the oxalate containing plants that cause poisoning in sheep and cattle.² Other plants that cause tubular necrosis include Easter lily in cats, *Quercus* spp. (oak) in ruminants, and *Amaranthus retroflexus* (pigweed) in pigs and cattle.² *Apergillus niger* and *flavus* can also produce enough oxalates to cause renal damage when ingested with feedstuffs.² Grapes and raisins cause tubular necrosis in dogs.²

Contributing Institution: Auburn University College of Veterinary Medicine (Dr. Koehler: jaw0007@auburn.edu)

References:

1. Haase M, Haase-Fielitz A, Bagshaw SM, Ronco C, Bellomo R: Cardiopulmonary bypass-associated acute kidney injury: a pigment nephropathy? *Contrib Nephrol* **156**:340-353, 2007
2. Schlafer DH, Miller, RB: Inflammatory Diseases of the Uterus. *In: Jubb, Kennedy, and Palmer's Pathology of Domestic Animals*, ed. Maxie, MG, 5th ed., vol. 2, pp 466-469. Elsevier, Philadelphia, USA, 2007
3. Zager RA, Gamelin LM: Pathogenetic mechanisms in experimental hemoglobinuric acute renal failure. *Am J Physiol* **256**:F446-F455, 1989

CASE II – Rabbit 2008 (AFIP 3106178)

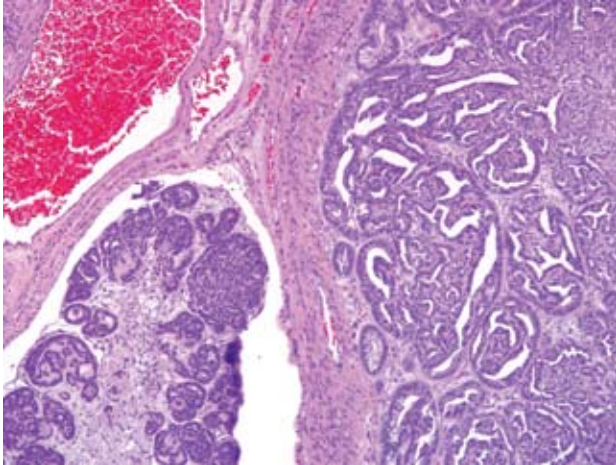
Signalment: Female rabbit (*Orytolagus cuniculus*), adult (unknown age)

History: The rabbit was found outdoors with a mammary mass (sub-Q mass about 5-6 cm diameter) in the caudal ventral abdomen that turned out to be a malignant hair follicle tumor. The uterus was removed at a later date because an abdominal mass was palpated and to spay the rabbit.

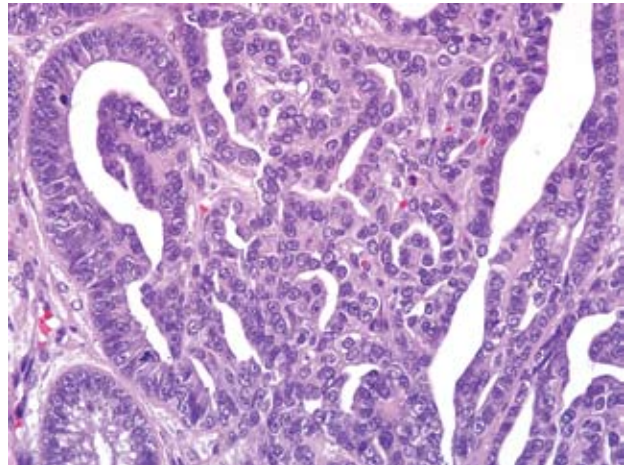
Gross Pathology: Firm pale masses, thickened friable mucosa, and multiple mucosal cysts.

Laboratory Results: NA

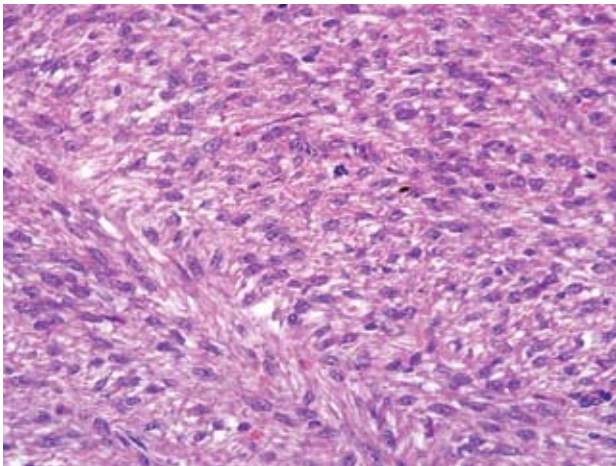
Histopathologic Description: Histologically, there are two distinctly different masses present within the same section adjacent to the mesometrial insertion;



2-1. Uterus, rabbit. Adenocarcinoma. Expanding the endometrium and infiltrating the myometrium is a neoplasm composed of polygonal cells arranged in tubules and papillary projections. Multifocally, there is lymphatic invasion by the neoplastic cells. (HE 200X)



2-2. Uterus, rabbit. Adenocarcinoma. Neoplastic cells are arranged on a fine fibrovascular stroma. Mitoses average 1 per 400X field. (HE 400X)



2-3. Uterus, rabbit. Leiomyosarcoma. Expanding the myometrium is a neoplasm composed of spindled cells arranged in short interlacing streams and bundles on a fine fibrovascular stroma. Mitoses average 2 per 400X field, and there are rare multinucleate neoplastic cells. (HE 400X)

the first located in the endometrium, the second located within the myometrium. The masses are located adjacent to one another and in some areas are in direct contact. The endometrial mass is multilobulated and well demarcated but unencapsulated. It is composed of thick papillary projections expanding into the uterine lumen, as well as lobules of densely packed tubular and glandular structures infiltrating into the subjacent myometrium (**Fig. 2-1**). Within the papillary projections and lobules, cuboidal to columnar neoplastic epithelial cells form a single, albeit crowded, layer supported by variable amounts of

loose vascular collagenous stroma (**Fig. 2-2**). Lobules are separated by moderate amounts of loose collagenous or myxomatous stroma, while within lobules, cells are supported by scant stroma. The neoplastic population has moderate anisocytosis and anisokaryosis. There are 1-3 mitotic figures per 400X field. Minimal amounts of sloughed cells, inflammation and necrosis are present within the mass. In some sections there are lobules of neoplastic cells within uterine lymphatic vessels covered by a layer of endothelium. Microscopic features of this mass are consistent with an adenocarcinoma.²

Microscopically, the second mass, located in the myometrium, is multilobulated, unencapsulated, poorly demarcated in some areas and infiltrative. It is composed of densely cellular, broad interlacing fascicles of medium sized spindloid cells (**Fig. 2-3**). These neoplastic cells have indistinct cytoplasmic borders, moderate amounts of vacuolated or fibrillar eosinophilic cytoplasm, a blunt-ended oval nucleus with finely granulated chromatin and a single eosinophilic nucleolus. In general, there is slight anisocytosis and anisokaryosis, however, rare karyomegalic and multinucleated cells are present. Mitotic figures are uncommon (1 per ten 400X fields). There are several large areas of necrosis with hemorrhage present within the mass (not present in all sections, Images 1 and 2). Although the mitotic rate is low and the neoplastic cells are well-differentiated, the presence of areas of necrosis is consistent with a diagnosis of leiomyosarcoma rather than leiomyoma.²

Contributor's Morphologic Diagnosis:

Uterus: Adenocarcinoma

Uterus: Leiomyosarcoma

Contributor's Comment: In contrast to other domestic species where uterine adenocarcinomas are a rare occurrence, the incidence of uterine adenocarcinomas has been reported to be up to 79% in female rabbits over the age of five years, with variation in breed predisposition. In fact, this tumor type is the most common tumor of *Orytolagus cuniculus* overall.⁶ Uterine adenocarcinomas in rabbits are often multicentric and affect both uterine horns.¹ Most are slow growing and present with bloody discharge and/or decreased fertility in breeding animals.^{5,6} The pathogenesis of these tumors is unclear and appears to be different from those occurring in humans, although there is controversy over this subject in the literature. Uterine leiomyosarcomas are much less common than adenocarcinomas with reported incidences of 1% in aging Dutch rabbits, and 2% in rabbits presenting to veterinarians with uterine disorders.^{1,5} The submitted case represents a simultaneous occurrence of two spontaneous uterine tumors in a female rabbit. Recently a similar case of concurrent adenocarcinoma and leiomyoma in an individual animal was reported by Kurotaki et al.⁴ The case report describes two endometrial adenocarcinomas, one of which was closely associated with a myometrial leiomyoma. These cases are similar in the presence of both primary epithelial and mesenchymal tumors within the uterus, with a close physical association between the two. They are different in that the smooth muscle tumor is malignant in the submitted case.

AFIP Diagnosis:

Uterus: Adenocarcinoma

Uterus: Leiomyosarcoma

Conference Comment: The cow is the only other domesticated animal that commonly gets uterine adenocarcinomas. This tumor is often seen in abattoirs and grossly appears as single or multiple firm masses in the wall of the uterus.³ These tumors are often umbilicated and are known to metastasize to the internal iliac lymph nodes and lungs.³ Histologically, this tumor often causes an intense fibrous response with numerous mitoses, cellular pleomorphism, and vascular and lymphatic invasion.³

Other differentials for a neoplastic growth in the uterus of domesticated animals include adenoma, fibroma, leiomyoma, and leiomyosarcoma as mentioned by the contributor. Adenomas are generally rare in domesticated species and can be difficult to distinguish from focal endometrial hyperplasia.³ Fibromas are generally firm, white, expansile masses that histologically appear as very bland, sparsely cellular, densely collagenous growths.³ Fibromas are seen most commonly in dogs and cattle, but

they are not prevalent tumors.³ Leiomyomas are composed of interwoven bundles of smooth muscle originating in the myometrium. The amount of connective tissue can be highly variable.³ These tumors are seen in dogs, cats, and cattle.³

Contributing Institution: Eli Lilly and Company, Greenfield IN

References:

1. Baba N, von Haam E: Animal Model: Spontaneous adenocarcinoma in aged rabbits. *Am J Path* **68**:653-656, 1972
2. Cooper BJ, Valentine BA: Tumors of Muscle. *In: Tumors of Domestic Animals*, ed Meuten DJ, 4th ed., 319-363, 2002
3. Kennedy PC, Cullen JM, Edwards JF, Goldschmidt MH, Larsen S, Munson L, Nielsen S: Histological classification of tumors of the genital system of domestic animals. *In: World Health Organization Histological Classification of Tumors of Domestic Animals*, ed. Schulman FY, Second Series, vol. 4, pp. 32-33, 72. Armed Forces Institute of Pathology, Washington, DC, 1999
4. Kurotaki T, Kokoshima H, Kitamori F, Kitamori T, Tsuchitani M: A case of adenocarcinoma of the endometrium extending into the leiomyoma of the uterus in a rabbit. *J Vet Med Sci* **69**:981-984, 2007
5. Saito K, Nakanishi M, Hasegawa A: Uterine disorders diagnosed by ventrotomy in 47 rabbits. *J Vet Med Sci* **64**(6):495-497, 2002
6. Weisbroth SH: Neoplastic Diseases. *In: The Biology of the Laboratory Rabbit*, eds. Manning PJ, Ringler DH, Newcomer CE, 2nd ed., 259-292, Academic Press, New York, NY, 1994

CASE III – 07-59363 (AFIP 3121220)

Signalment: 6-month-old, male, domestic ferret (*Mustela putorius furo*)

History: This 6-month-old, male domestic ferret presented to the referring veterinarian with a 1-2 week history of diarrhea and lethargy. On physical exam, the animal was assessed as being moderately dehydrated. The abdomen was moderately distended. Abdominal ultrasound showed marked enlargement of the spleen, multifocal areas of hyperechogenicity in the liver, and markedly enlarged mesenteric lymph nodes. Over the next week, diarrhea

continued and the ferret became anorexic, lost weight, and developed a mild cough despite symptomatic treatment. Euthanasia was elected and the animal was submitted to the Diagnostic Center for Population and Animal Health, Lansing, MI for necropsy.

Gross Pathology: On gross necropsy, the animal was in fair to poor body condition with no visible fat stores and increased prominence of bony protuberances. Dehydration was marked as evinced by retraction of the eyes into the orbits and tackiness of visceral surfaces. The abdomen was prominently distended due to marked enlargement of the spleen and mesenteric lymph nodes. The spleen was approximately 10 times normal size, dark black and diffusely meaty. There were 7-8 relatively indistinct, poorly circumscribed, pale white, semi-firm, nodular foci dispersed throughout the splenic parenchyma. These foci ranged from 0.5-1.5 cm in maximum diameter, and the capsular surface of the spleen overlying few of these areas was slightly raised. The liver was diffusely mottled dark red and tan, and was mildly enlarged with slightly rounded borders. There were 10-12 slightly raised, occasionally coalescing, pale white, firm, slightly nodular plaques ranging from 0.5-1 cm in diameter randomly distributed on the capsular surface of the liver. The mesenteric lymph nodes were markedly enlarged being approximately 5-8 times normal size. The capsular surfaces of lymph nodes were irregular due to dozens of 2-5 mm in diameter, slightly raised white nodules. On cut surface, the normal nodal architecture was obliterated by pale tan to white, firm tissue (**Fig. 3-1**). The mesentery was irregularly thickened

by dozens of coalescing pale white, firm nodules and irregular plaques. Similar white nodules and plaques were segmentally distributed across the serosal surfaces of the jejunum, ileum and to a lesser degree colon. In few areas, sections of intestinal loops were adhered to each other and to adjacent mesenteric lymph nodes by both fibrinous and fibrous adhesions. The visceral pleural surfaces of the lung were focally raised 1-3 mm by similar irregularly shaped, pale white, poorly demarcated, firm plaques that ranged from .2-1.5 cm in diameter. No other significant lesions were noted grossly.

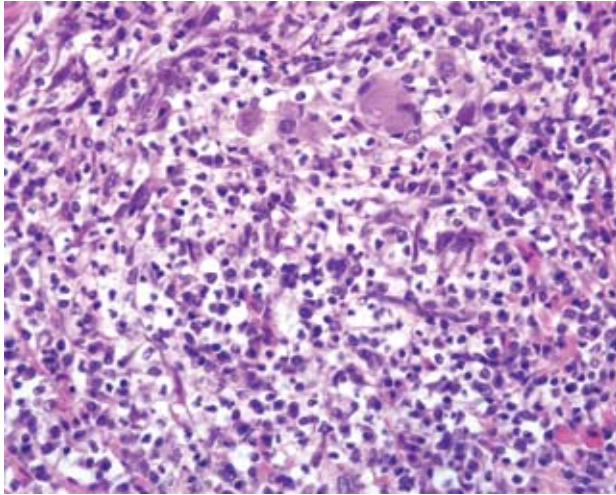
Laboratory Results: PCR for Aleutian mink disease virus was negative.

Histopathologic Description: The submitted slides represent small intestine and/or lymph node.

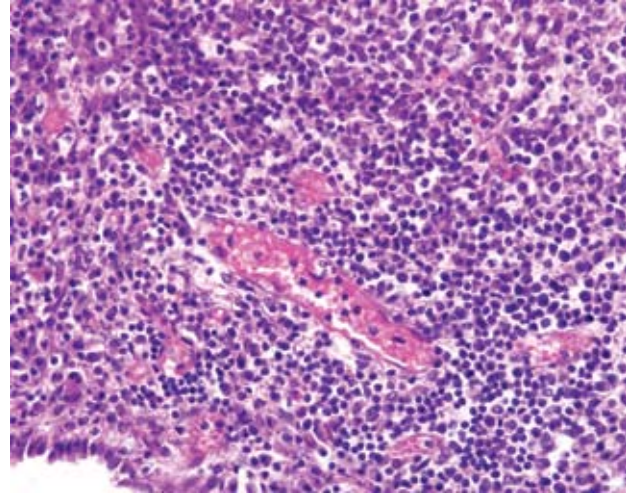
In the wall of the small intestine, there are multifocal to coalescing areas of granulomatous to pyogranulomatous inflammation. These areas are most prominent on the serosal surfaces of the intestine, but also extend into the underlying tunic muscularis and more rarely into the submucosa and mucosa. Granulomas and pyogranulomas are characterized by variable central necrosis and infiltrates of degenerate neutrophils surrounded by thick dense bands of plump epithelioid macrophages and rare multinucleated foreign body type giant cells. Varying rings of lymphocytes, plasma cells, and dense maturing fibrosis surround granulomas. Granulomatous inflammation is generally randomly distributed, but



3-1. Mesenteric lymph node, ferret. Lymph nodes are markedly enlarged and nodal architecture on cut surface is obliterated by pale tan to white firm tissue. Photograph courtesy of Diagnostic Center for Population & Animal Health, 4125 Beaumont Road, Lansing, MI 48910, fitzgerald@dcpah.msu.edu.



3-2. Mesenteric lymph node, ferret. Nodal architecture is effaced by pyogranulomatous inflammation with few multinucleate giant cells and scattered fibroblasts. (HE 400X)



3-3. Small intestine, ferret. Multifocally surrounding vasculature near areas of pyogranulomatous inflammation are large numbers of lymphocytes and plasma cells and fewer histiocytes. (HE 400X)

occasionally is associated with vasculature. In sections of lymph node, nodal architecture is expanded and ablated by multifocal and coalescing granulomas and pyogranulomas similar to those described in the small intestine (**Fig. 3-2**). Granulomatous inflammation extensively extends through the capsule into the surrounding perinodal adipose tissue. Similar foci of granulomatous to occasionally pyogranulomatous inflammation expand the serosal surfaces of the liver and lung, and focally obliterate the normal parenchyma of the lung and spleen. In rare areas, the meninges overlying the cerebral cortex are expanded by granulomatous inflammation. Vasculature within tissue surrounding foci of granulomatous inflammation in the liver, lung, and cerebral cortex is segmentally surrounded by moderate cuffs of lymphocytes, plasma cells, and fewer histiocytes (**Fig. 3-3**). Immunohistochemistry using a generic antibody against Group 1 coronaviruses on sections of small intestine, lymph node, lung, and spleen demonstrated strong positive, intracytoplasmic immunoreactivity within macrophages at the center of granulomas. A generic coronavirus RT-PCR yielded amplification of a 650 base pair fragment. Sequencing of this segment suggests that the amplified virus is distinct from feline coronavirus (FeCoV). The amplified virus appears to be most closely related to ferret enteric coronavirus (FECV) that reportedly causes epizootic catarrhal enteritis (ECE) in ferrets.

Contributor's Morphologic Diagnosis: Small intestine: Severe chronic segmental granulomatous to pyogranulomatous enteritis and peritonitis

Lymph node: Severe chronic multifocal and coalescing

granulomatous to pyogranulomatous lymphadenitis

Contributor's Comment: This case presentation represents a disease that has been termed granulomatous inflammatory syndrome (GIS) or ferret systemic coronavirus infection (FSCV).^{1,4} This is an emerging disease in ferrets that was first reported in the veterinary literature in 2006 and closely resembles the clinical, gross and microscopic features of feline infectious peritonitis.^{1,2,4}

The exact etiopathogenesis of this lesion is unclear at this point, but appears to be related to infection with a group 1 coronavirus. Immunohistochemistry using monoclonal antibodies against feline coronavirus (FCoV) has been reported to demonstrate immunoreactivity in macrophages within lesions.^{1,2} This antibody is not specific for FCoV as it has been shown to detect other group 1 coronaviruses including ferret enteric coronavirus (FECV) that has been implicated as the cause of epizootic catarrhal enteritis (ECE).^{5,6} Electron microscopy confirmed the presence of coronavirus-like particles within macrophages.¹ RT-PCR using primers that detect a broad array of group 1 coronaviruses yielded amplification of a 599bp sequence that showed significant similarity to FECV (77% homology) and to other group 1 coronaviruses.¹ Whether this virus represents a novel virus or variation within an already described coronavirus is unclear. The exact mechanism by which this virus causes the described lesions is unknown. Further characterization of the virus is required.

AFIP Diagnosis: Small intestine: Enteritis and peritonitis, pyogranulomatous, multifocal to coalescing, moderate

Lymph node: Lymphadenitis, pyogranulomatous, multifocal to coalescing, moderate

Conference Comment: Coronaviruses are single-stranded RNA viruses of major importance in domestic animals.³ Coronaviruses are currently split into 3 serogroups. Group 1 includes transmissible gastroenteritis of swine (TGEV), canine coronavirus (CCV), feline coronavirus (FCoV), and human coronavirus 229E. Mouse hepatitis virus, sialodacryoadenitis of rats, turkey coronavirus ("bluecomb"), and bovine coronavirus are the major viruses recognized in group 2.^{1,3} Group 3 comprises the avian viruses and includes infectious bronchitis virus.^{1,3} As the contributor mentioned, ferret systemic coronavirus infection (FSCV) has an almost identical gross and histologic appearance as FIP in domestic cats. Juvenile and young adult ferrets seem to be the most susceptible to this disease.⁽¹⁾ Gross lesions consist of widespread nodular foci on multiple serosal surfaces that closely resemble similar foci seen in clinical cases of FIP.¹ Involvement of mesenteric lymph nodes is also reminiscent of FIP in cats. FSCV closely resembles the dry form of FIP.¹ Histologic lesions are identical to what is seen in cats with FIP and consist of pyogranulomatous inflammation with vasculitis and perivasculitis.¹ Relevant clinical pathologic findings in these ferrets included a mild non-regenerative anemia (anemia of chronic disease), thrombocytopenia and hyperproteinemia.¹ The thrombocytopenia was attributed to DIC secondary to vasculitis, while the hyperproteinemia occurred due to hyperglobulinemia.¹

Contributing Institution: Michigan State University, Diagnostic Center for Population and Animal Health, 4125 Beaumont Rd, Lansing, MI 48910 www.animalhealth.msu.edu

References:

1. Garner MM, Ramsell K, Morera N, Juan-Sallés C, Jiménez J, Ardiaca M, Montesinos A, Teifke JP, Löhr CV, Evermann JF, Baszler TV, Nordhausen RW, Wise AG, Maes RK, Kiupel M. Clinicopathologic features of a systemic coronavirus-associated disease resembling feline infectious peritonitis in the domestic ferret (*Mustela putorius furo*). *Vet Pathol* **45**(2):236-46, 2008
2. Martínez J, Ramis AJ, Reinacher M, Perpiñán D. Detection of feline infectious peritonitis virus-like antigen in ferrets. *Vet Rec* **158**:523, 2006
3. Murphy FA, Gibbs EPJ, Horzinek MC, Studdert MJ: Coronaviridae. In: *Veterinary Virology*, 3rd ed., pp. 495-508. Academic Press, San Diego, California, 1999
4. Perpiñán D, López C. Clinical aspects of systemic

granulomatous inflammatory syndrome in ferrets (*Mustela putorius furo*). *Vet Rec* **162**(6):180-185, 2008

5. Williams B, Kiupel M, West K, Raymond JT, Grant CK, Glickmann LT, Coronavirus associated enzootic catarrhal enteritis (ECE) in ferrets (*Mustela putorius furo*): a review of 120 cases (1993-1998) *JAVMA* **217**: 526-530, 2000

6. Wise AG, Kiupel M, Maes RK. A novel coronavirus associated with epizootic catarrhal enteritis (ECE) in ferrets. *Virology* **349**:164-174, 2006

CASE IV – S08-0692 (AFIP 3103039)

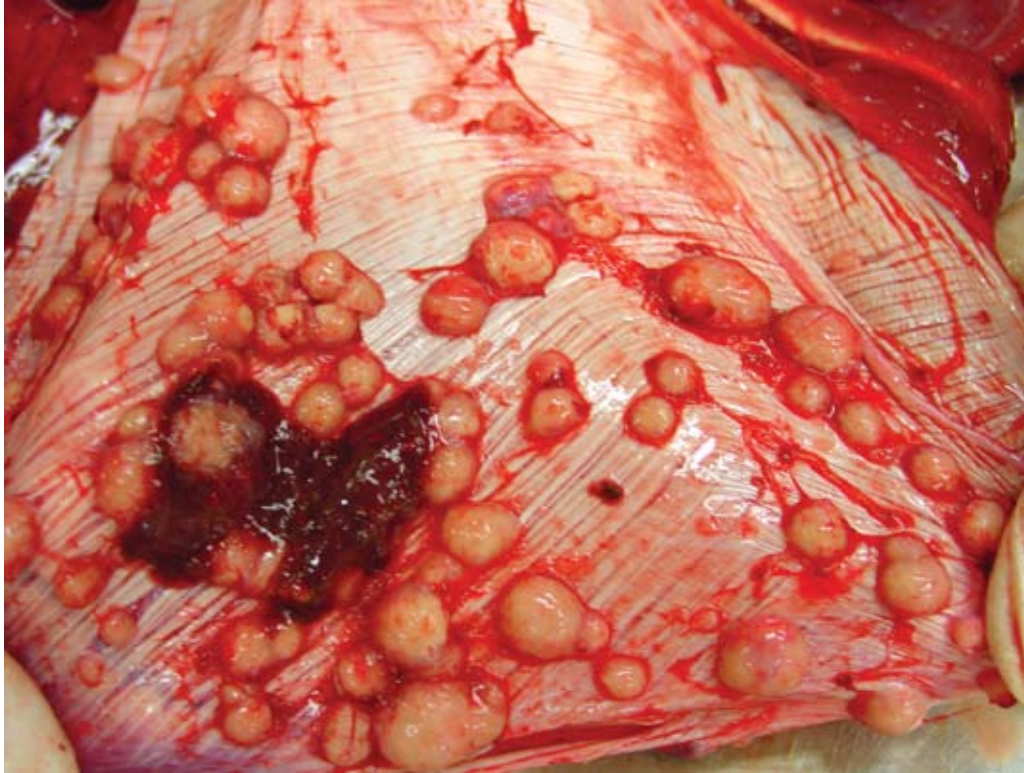
Signalment: 10-year-old, female, (*Lama pacos*) Alpaca

History: The animal was presented to the clinicians of the Institute of Farm Animals of the University of Zurich because of cachexia and weakness although it seemed to be eating normally. Clinical findings were intensified breathing, weakness and loss of gastrointestinal motility. The sonographic picture of the liver showed multifocal, echogenic, round to sickle-shaped unencapsulated structures of about 1 to 3 cm in diameter.

Gross Pathology: Firm, whitish nodules in size from 1 to 7 centimeters in diameter were found in the liver, lung, mediastinum, pleura, and omentum (**Figs. 4-1, 4-2**). In the cut surface some of the nodules showed fine whitish to grey beige spikes which were arranged in radial patterns (**Fig. 4-3**), other nodules showed centrally located homogenous grey beige caseous material with multifocal white gritty spots (**Fig. 4-4**).

Laboratory Results: Acid-fast stain (Ziehl-Neelson stain) revealed myriads of acid-fast bacteria in epithelioid macrophages and the PCR analysis resulted in *Mycobacterium kansasii*.

Histopathologic Description: Liver: Up to 70% of the parenchyma is replaced by multifocal to coalescing granulomas characterized by an amorphous, eosinophilic necrosis material surrounded by a smaller layer of elongated macrophages with light eosinophilic cytoplasm, a centrally located oval nucleus and indistinct cell borders (epithelioid cells) and rarely of large cells with eosinophilic cytoplasm and numerous nuclei located



4-1. Pleura, alpaca. Adherent to the pleura are multiple granulomas.

Photograph courtesy of Institute of Veterinary Pathology, Winterhurerstrasse 268, 8057 Zuerich, Switzerland, grest@vetpath.uzh.ch.

in the periphery of the cell (multinucleated giant cells, Langhans-type) which are once again surrounded by a rim of lymphocytes, plasma cells, macrophages, fibroblasts embedded in a small amount of collagen fibers and to a lesser extent neutrophils (Fig. 4-5). Multifocally necrotic areas contain dark basophilic granular material (dystrophic calcification). The liver parenchyma is diffusely infiltrated with a moderate amount of lymphocytes and neutrophils.

Contributor's Morphologic Diagnosis: Liver, granulomatous hepatitis, multifocal and coalescing, severe, chronic, with central caseous necrosis and myriads of acid-fast intrahistiocytic rod shaped bacteria (Fig. 4-6) (*Mycobacteria kansasii*)

Contributor's Comment: *Mycobacterium kansasii* is classified in Runion's Group 1 and belongs to the nontuberculous mycobacteria (NTM); or mycobacteria other than tuberculosis (MOTT). It is a saprophyte which is found in soil and water. *M. kansasii* is very heterogeneous as 5 well-defined different types (I-V) exist of which type I is frequently isolated from humans, type II from humans and the environment and III-V were present mostly in the environment and only rarely in humans sources.² *M. kansasii* infection is described in cattle to cause lesions similar to bovine tuberculosis (BTB) although it seems to be exceedingly rare.^{5,6} In slaughtered cattle in Great

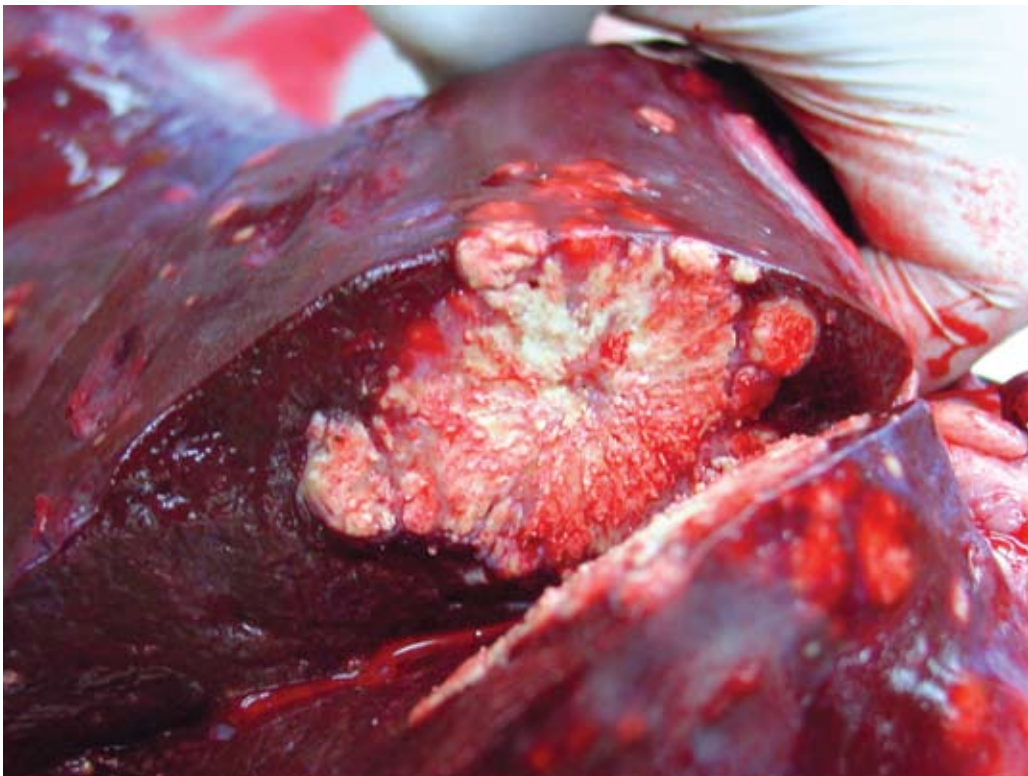
Britain an incidence of 0.8% NTM was found and the majority of these belong to the *M. avium* complex.⁵ In Northern Ireland *M. kansasii* could be detected in 14 tissue specimens of 16,506 cattle, which demonstrates the rareness of the disease in cattle. Nevertheless, it is not known how many animals that are exposed to *M. kansasii* do not develop disease. It was also found that *M. kansasii* could be isolated from humans without disease.⁵ However, *M. kansasii* can cause pulmonary or disseminated disease in humans with an estimated 300 times higher incidence in HIV- patients.² Experimental infection of healthy cattle failed to cause disease or pathologic changes but it did induce immune responses in TB tests.⁶ Since, some NTM and specifically *M. kansasii* do share some diagnostic antigens with *Mycobacterium bovis* complex bacteria^{4, 5} there can be cross-reactions in traditional TB tests, which complicates the control and eradication of BTB.

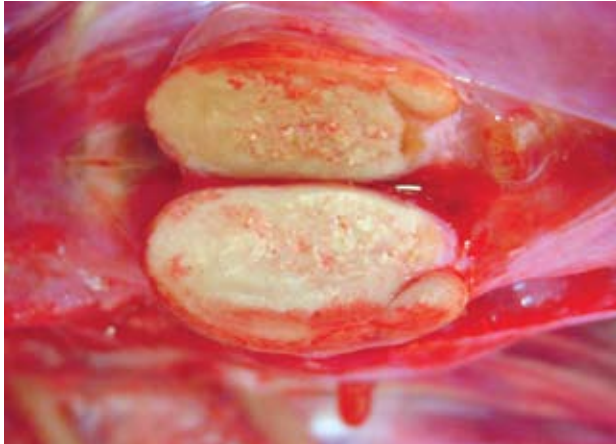
AFIP Diagnosis: Liver: Granulomas, multifocal to coalescing, with mild hepatocellular degeneration

Conference Comment: Mycobacteria are gram-positive bacteria with high lipid content within their cell wall. This makes traditional gram staining largely ineffective, but mycobacteria do stain with carbol-fuchsin and resist decoloration by inorganic acids giving them their "acid-fast" staining characteristic.³ Mycolic acid

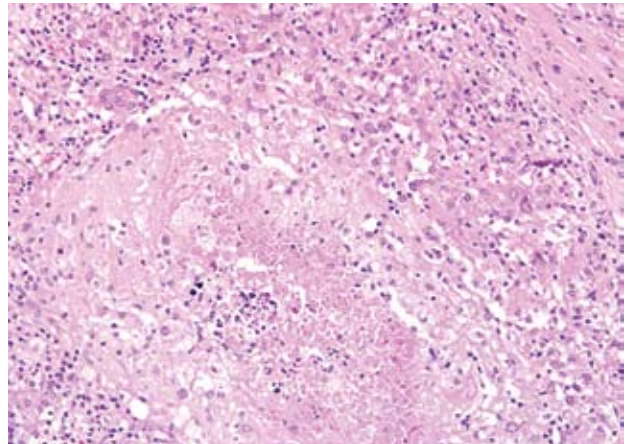


4-2., 4-3. Liver, alpaca. Expanding the hepatic parenchyma are multifocal to coalescing granulomas. On cut surface, granulomas have radiating streaks of mineral which surround a central area of necrosis. Photographs courtesy of Institute of Veterinary Pathology, Winterhurerstrasse 268, 8057 Zuerich, Switzerland, grest@vetpath.uzh.ch.





4-4. Lymph node, alpaca. Normal nodal architecture is effaced by a large granuloma which contains granular foci of mineral. Photograph courtesy of Institute of Veterinary Pathology, Winterthurerstrasse 268, 8057 Zuerich, Switzerland, grest@vetpath.uzh.ch.



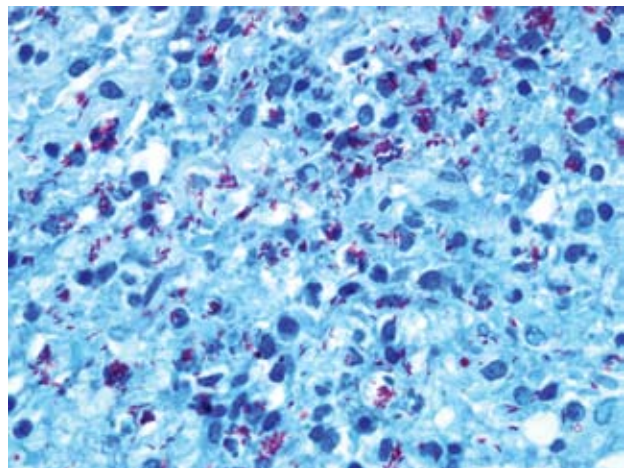
4-5. Liver, alpaca. Granulomas are composed of a central core of necrosis and mineral which are bounded by moderate numbers of epithelioid macrophages and fewer multinucleate giant cells, further bounded by lymphocytes and plasma cells admixed with few fibroblasts. (HE 400X)

spacing within the bacterial cell wall is key to these bacteria being acid-fast.³ These same mycolic acids are hydrophobic accounting for the environmental hardiness and antimicrobial resistance of these troublesome bacteria.³ During the conference, Colonel Raymond questioned the participants about the classifications of mycobacteria and then the mechanistic basis of tuberculin skin testing. These bacteria cause a type IV hypersensitivity reaction, or delayed type hypersensitivity, as demonstrated by the tuberculin test. Histologically this manifests as aggregates of mononuclear cells around small veins and venules, or perivascular inflammation and cuffing.¹ Important cytokines involved in delayed type hypersensitivity reactions include IL-12, IL-2, IFN-gamma, and TNF. IL-12 is critical in propagating a Th1 response, IL-2 causes an autocrine and paracrine proliferation of T cells, and IFN-gamma is a potent macrophage activator.¹ TNF is an important cytokine that acts on endothelial cells to cause vasodilation and facilitates the process of adhesion and extravasation of lymphocytes and monocytes.¹

Contributing Institution: Institute of Veterinary Pathology, University of Zürich, Winterthurerstrasse 268, CH-8057 Zürich, Switzerland.

References:

1. Abbas, Abul K: Disease of Immunity. *In: Robins and Cotran Pathologic Basis of Diseases*, ed. Kumar VK, Abbas AK, Fausto N, 7th ed., pp. 216-218. Elsevier, Philadelphia, Pennsylvania, 2005
2. Alcaide F, Richter I, Bernasconi C, Springer B, Hagenau C, Schulze-Röbbecke R, Tortoli E, Martin R, Böttger EC, Telenti A: Heterogeneity and clonality



4-6. Liver, alpaca. Within granulomas are numerous free and intrahistiocytic, 1x3 um, filamentous, acid fast bacteria. (Fite-Faraco 1000X)

among isolates of *Mycobacterium kansasii*: implications for epidemiological and pathogenicity studies. *J Clin Microbiol* 35(8):1959-64, 1997

3. Caswell JL, Williams KJ: Respiratory system. *In: Jubb, Kennedy and Palmer's Pathology of Domestic Animals*, ed. Maxie MG, 5th ed., pp. 632. Elsevier, Philadelphia, Pennsylvania, 2007

4. Huges MS, Ball NW, McCarroll J, Erskine M, Taylor MJ, Pollock JM, Skuce RA, Neill SD: Molecular analysis of mycobacteria other than the *M. tuberculosis* complex isolated from Northern Ireland cattle. *Vet microbiol* 108:101-112, 2005

5. Vordermeier HM, Brown J, Cockle OJ, Franken WPJ,

Arend SM, Ottenhoff THM, Jahans K, Hewinson RG: Assessment of cross-reactivity between *Mycobacterium bovis* and *M. kansasii* ESAT-6 and CFP-10 at the T-cell epitope level. Clin Vaccine Immunol **14**(9):1203-9, 2007

6. Waters WR, Palmer MV, Thacker TC, Payeur JB, Harris NB, Minion FC, Greenwald R, Esfandiari J, Andersen P, McNair J, Pollock JM, Lyashchenko KP: Immune responses to defined antigens of *Mycobacterium bovis* in cattle experimentally infected with *Mycobacterium kansasii*. Clin Vaccine Immunol **13**:611-9, 2006